

CHARACTERIZING THE COOL KEPLER OBJECTS OF INTEREST. NEW EFFECTIVE TEMPERATURES, METALLICITIES, MASSES AND RADII OF LOW-MASS KEPLER PLANET-CANDIDATE HOST STARS

PHILIP S. MUIRHEAD^{1,2}, KATHERINE HAMREN³, EVERETT SCHLAWIN, BÁRBARA ROJAS-AYALA⁴, KEVIN R. COVEY⁵, JAMES P. LLOYD

Department of Astronomy, Cornell University, 122 Sciences Drive, Ithaca, NY 14853, USA

(Dated:)

Draft version February 5, 2022

ABSTRACT

We report stellar parameters for late-K and M-type planet-candidate host stars announced by the Kepler Mission. We obtained medium-resolution, K-band spectra of 84 cool ($T_{\text{eff}} \lesssim 4400$ K) Kepler Objects of Interest (KOIs) from Borucki et al. We identified one object as a giant (KOI 977); for the remaining dwarfs, we measured effective temperatures (T_{eff}) and metallicities $[M/H]$ using the K-band spectral indices of Rojas-Ayala et al. We determine the masses (M_{\star}) and radii (R_{\star}) of the cool KOIs by interpolation onto the Dartmouth evolutionary isochrones. The resultant stellar radii are significantly less than the values reported in the Kepler Input Catalogue and, by construction, correlate better with T_{eff} . Applying the published KOI transit parameters to our stellar radius measurements, we report new physical radii for the planet candidates. Recalculating the equilibrium temperatures of the planet-candidates assuming Earth's albedo and re-radiation fraction, we find that 3 of the planet-candidates are terrestrial-sized with orbital semi-major axes that lie within the habitable zones of their host stars (KOI 463.01, KOI 812.03 and KOI 854.01). The stellar parameters presented in this letter serve as a resource for prioritization of future follow-up efforts to validate and characterize the cool KOI planet candidates.

Subject headings: Planetary Systems — Stars: fundamental parameters — Stars: abundances — Stars: late-type — Stars: low-mass

1. INTRODUCTION

Estimating physical parameters of stars which host exoplanets is crucial for estimating the physical parameters of the exoplanets themselves. The wealth of detailed observations of the Sun has enabled precise calibration of stellar evolution models for Sun-like stars, such that the determination of fundamental stellar physical parameters (mass, effective temperature, luminosity, radius) from observed colors and spectra is routine and generally robust (e.g. Kurucz 1991; Nordström et al. 2004; Valenti & Fischer 2005).

For cool dwarfs ($T_{\text{eff}} \lesssim 4400$ K, $M \lesssim 0.5 M_{\odot}$), however, the situation is more complex. Low-mass stellar models are not as well calibrated, and their predictions differ substantially depending on assumptions such as the mixing length parameter. There are few M dwarfs that are bright enough and nearby enough for direct accurate parallax and radius measurements (e.g. Ségransan et al. 2003; Berger et al. 2006). Eclipsing binaries have been the primary source of radii for M dwarfs, but there is a discrepancy between observed radii and predictions from stellar evolution models (Ribas 2006; Torres 2011). The rapid rotation of these close binary systems may

be responsible for the discrepancy; however magneto-hydrodynamic effects may suppress convection in their interiors, so these radii may not be representative of field objects (Chabrier et al. 2007; Kraus et al. 2011).

Recently, M dwarfs have received increased attention in both transit and radial velocity searches for exoplanets (e.g. Charbonneau et al. 2009; Bean et al. 2010b; Johnson et al. 2010; Mahadevan et al. 2010; Muirhead et al. 2011; Bonfils et al. 2011), and exoplanet characterization efforts (e.g. Bean et al. 2010a; Désert et al. 2011; Croll et al. 2011), thanks to the higher detectability and characterization signals from orbiting low-mass exoplanets (Nutzman & Charbonneau 2008). In February of 2011 the Kepler Mission announced 997 objects whose light curves are consistent with the presence of transiting planets (Borucki et al. 2011), 74 of these Kepler Objects of Interest (KOIs) have $T_{\text{eff}} < 4400$ K in the Kepler Input Catalog (KIC; Batalha et al. 2010; Brown et al. 2011). A statistical analysis of the KOIs by Howard et al. (2011) reveals a substantial rise in the frequency of short-period, 2-4 R_{\oplus} planets with decreasing T_{eff} of their host stars, implying that the low-mass planet candidates detected around low-mass stars represent a ubiquitous population of planets in the Galaxy.

Stellar parameters in the KIC were inferred from a photometric survey of stars in the Kepler field-of-view. However, Brown et al. (2011) state that the KIC stellar parameters are reliable for Sun-like stars, but are “untrustworthy” for stars with T_{eff} less than 3750 K. The most reliable estimates of M dwarf masses and radii are derived by combining measured stellar luminosities with reliable mass-luminosity relations (e.g. Delfosse et al. 2000) and

¹ Current address: Department of Astronomy, California Institute of Technology, 1200 East California Boulevard, MC 249-17, Pasadena, CA 91125, USA

² philm@astro.caltech.edu

³ Current address: Department of Astronomy and Astrophysics, University of California Santa Cruz, 1156 High Street, Santa Cruz, CA 95064, USA

⁴ Current address: Department of Astrophysics, American Museum of Natural History, Central Park West at 79th Street, New York, NY 10024, USA.

⁵ Hubble Fellow

mass-radius relations predicted by stellar evolutionary models (e.g. Baraffe et al. 1998), often with corrections to account for discrepancies between measured and predicted radii (e.g. Torres 2007). Unfortunately, the low-mass KOIs do not have parallax measurements, which are necessary to estimate stellar luminosity and hence mass and radius with these methods.

Near-infrared spectroscopy offers a more robust method for determining physical parameters for low-mass stars that lack parallax measurements. The K -band (2.0 to 2.4 μm) contains several useful spectral diagnostics including continuum regions sensitive to T_{eff} (Covey et al. 2010) and absorption features that are sensitive to stellar metallicity (Rojas-Ayala et al. 2010, 2012), with minimal sensitivity to interstellar reddening.

In this letter we report T_{eff} and $[M/H]$ measurements of 84 low-mass KOIs using K -band spectroscopy. We interpolated T_{eff} and $[M/H]$ onto the Dartmouth evolutionary isochrones (Dotter et al. 2008; Feiden et al. 2011), which reproduce measurements from optical long-baseline interferometry (OLBI) relatively well (see Figure 2) and contain a large spread of metallicity grid-points, as required for reliable interpolation of stellar parameters. We report interpolated stellar masses and radii of the low-mass KOIs, and recalculate the planetary parameters based on the transit parameters in Borucki et al. (2011).

2. OBSERVATIONAL CLASSIFICATION

2.1. Observations

Observations were carried out with the TripleSpec Spectrograph at the Palomar Observatory 200-inch Hale Telescope. TripleSpec is a near-infrared slit-spectrograph covering 1.0 to 2.5 μm simultaneously with a resolution of 2700 (Herter et al. 2008). Two positions on the slit, A and B, were used for each target, and exposures were taken in an ABBA pattern with 60 second integration times at each position. Multiple ABBA sets were taken and combined until each spectrum had a median per-channel signal-to-noise of at least 60.

For telluric calibration we used SIMBAD to identify a grid of A0V stars in the Kepler field-of-view, and developed an observing sequence such that each KOI observation has a corresponding A0V star observation taken within 40 minutes and with an airmass difference less than 0.1.

2.2. Target Selection

We observed all of the KOIs with KIC-ascribed effective temperatures less than 4400 K over 7 nights in June of 2011. Of the 74 KOIs, 4 appeared to be double objects in the TripleSpec slit viewer with separations of less than 6 arcseconds (roughly the size of the Kepler Spacecraft’s point spread function): KOI 326, KOI 641, KOI 249 and KOI 51. KOI 667 consisted of 5 objects within a 6 arcsecond radius. These objects are not included in this survey.

In August of 2011 we observed 15 additional KOIs with KIC-ascribed T_{eff} greater than 4400 K, but with colors indicative of low-mass stars: $(J - K) > 0.7$, $(r - i) > 0.3$, or $(g - r) > 1.0$. We include 13 of these KOIs in this letter, as their spectra revealed CO features indicative of low-mass stars. In total, we obtained spectra of 82 KOIs.

2.3. Data Reduction

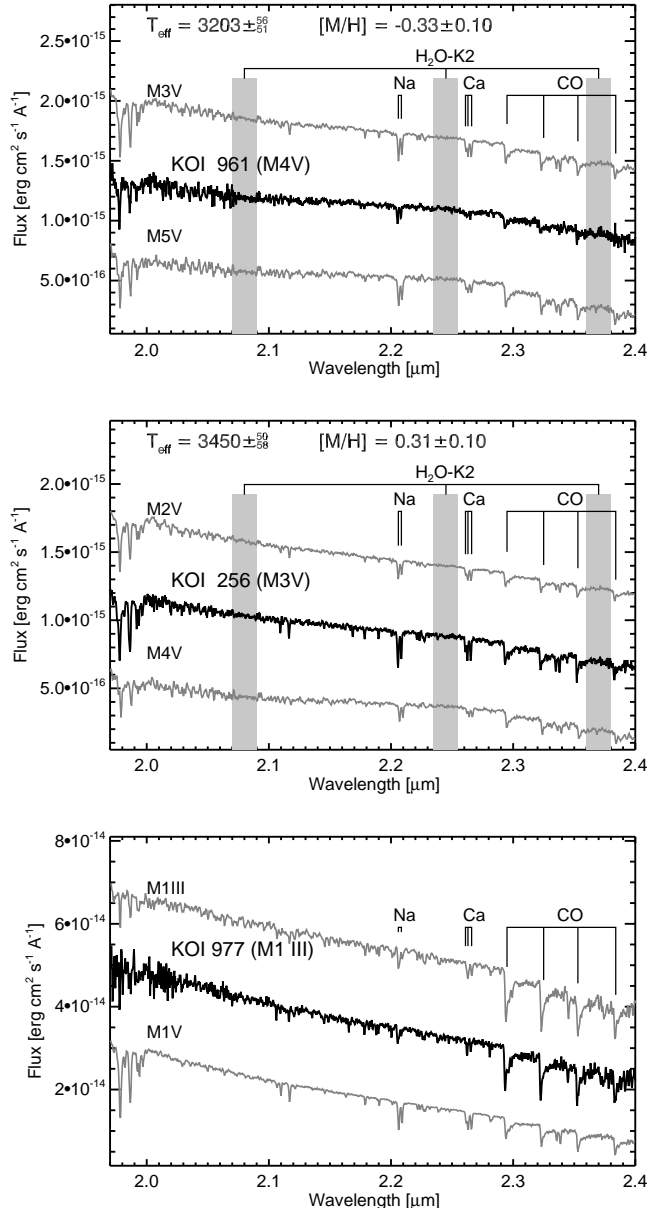


FIG. 1.— Palomar-TripleSpec K -band spectra of cool KOIs (black) with comparison KHM spectral type standards from the IRTF Spectral Library (gray, Cushing et al. 2005; Rayner et al. 2009). The templates are adjusted to the same scale as the KOI spectra using a ratio of the median flux in K band, and then artificially offset. We used the $\text{H}_2\text{O-K2}$ index to compute T_{eff} , which is calculated using regions dominated by water opacity, and we used the equivalent widths of the Na I doublet and Ca I triplet to measure $[M/H]$ (Rojas-Ayala et al. 2012). *Top*: KOI 961 is an example of a metal-poor star with little Na I and Ca I absorption (Muirhead et al. 2012). *Middle*: KOI 256 is an example of a metal-rich star with deep Na I and Ca I absorption. The metallicities $[M/H]$ are included, with uncertainties accounting for both random and systematic errors. *Bottom*: KOI 977 has a spectrum indicative of a giant with deep CO features but relatively weak Na I and Ca I absorption.

The spectra were extracted using a version of the Spextool program modified for the Palomar TripleSpec Spectrograph (Cushing et al. 2004, ; M. Cushing, private communication 2011). Spextool accepts data in ABBA format. The `xtellcor` package within Spextool accepts spectra of A0 stars and compares them to a model spec-

trum of Vega to identify and remove telluric absorption lines in a target spectrum (Vacca et al. 2003). Figure 1 plots three example spectra, with templates of similar spectra type and relevant spectral features indicated. The templates are taken from the IRTF Spectral Library (Cushing et al. 2005; Rayner et al. 2009).

One star in our sample has a K-band spectrum consistent with a giant star, suggesting that the observed light curve is due to a stellar, rather than planetary, companion, or that the transit signal is due to an unresolved blend with an eclipsing binary. KOI 977 shows weak Na I and Ca I absorption and strong CO absorption, which qualitatively match IRTF template spectra of giant stars but not dwarf stars of the same spectral type. The spectrum is included in Figure 1, with a giant and dwarf template for comparison.

3. MEASUREMENT OF T_{EFF} AND $[M/H]$

To measure T_{eff} and $[M/H]$ of the remaining dwarfs, we measured three spectral indices from the K-band spectra: the equivalent widths of the Na I and Ca I lines, at 2.210 and 2.260 μm respectively, and an index describing the change in flux between three 0.02 μm -wide bands dominated by water opacity—centered at 2.245, 2.370, 2.080 μm —called the H₂O-K2 index. Rojas-Ayala et al. (2012) describe the measurement of the Na I and Ca I equivalent widths, introduce H₂O-K2 index, and derive relations between the spectral indices and T_{eff} , overall metallicity ($[M/H]$) and KHM spectral type.

Briefly, we note that the Rojas-Ayala et al. (2012) $[M/H]$ relation was calibrated empirically using nearby M dwarfs with F, G or K-type binary companions that have SPOCS $[M/H]$ measurements (Valenti & Fischer 2005). Metallicity measurements for stars earlier than M0 ($T_{\text{eff}} \gtrsim 4000$ K) represent an extrapolation of the M dwarf $[M/H]$ calibration. The T_{eff} is calculated by interpolating the $[M/H]$ measurement and H₂O-K2 index onto a theoretical surface of T_{eff} versus $[M/H]$ and H₂O-K2 index calculated to the BT-settl late-type model spectra of Allard et al. (2011). To validate the T_{eff} measurement method, we compare T_{eff} measurements by Rojas-Ayala et al. (2012) to measurements from optical long-baseline interferometry in Figure 3, Panel A.

The T_{eff} surface is very metallicity insensitive ($< 10\text{K}$ offsets due to metallicity effects) for $3200 < T_{\text{eff}} < 3900$, and $[M/H] < 0.3$. For higher temperatures the H₂O-K2 index saturates, where the saturation T_{eff} depends on $[M/H]$. For stars with H₂O-K2 near the saturation, a slightly higher H₂O-K2 index converts to a large increase in the measured T_{eff} . We accommodate this by providing asymmetric uncertainty estimates in T_{eff} using a Monte Carlo approach described in Section 5. KOI 904 and KOI 956 had H₂O-K2 outside of the calculated surface, and are therefore not included in our results.

4. DETERMINATION OF MASS AND RADIUS

We place the low-mass KOIs on a grid of physical parameters based on the Dartmouth stellar evolution models (Dotter et al. 2008; Feiden et al. 2011). These models are in generally good agreement with OLBFI observations (see Figure 2), but there may well be systematic offsets in mass, radius or effective temperature, so these inferred physical parameters should be used with caution. We do not use the BCAH evolution models, as they are only

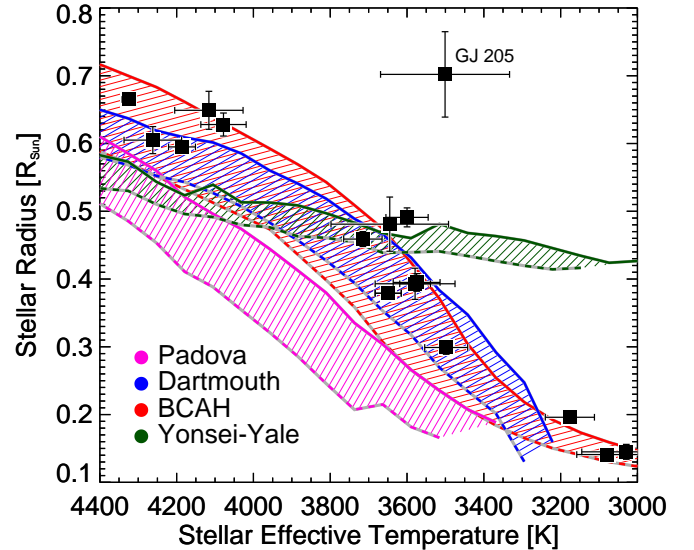


FIG. 2.— Predicted R_* versus T_{eff} for the 5-Gyr isochrones of Padova (Girardi et al. 2002), Dartmouth (e.g. Dotter et al. 2008; Feiden et al. 2011), Yonsei-Yale (Yi et al. 2003), and BCAH (Baraffe et al. 1998), for metallicities between $[M/H] = -0.5$ (dashed lines) and $[M/H] = 0.0$ (solid lines). We include empirical measurements of R_* and T_{eff} for low-mass field stars using optical long-baseline interferometry (OLBFI), with values taken from the literature (Berger et al. 2006; van Belle & von Braun 2009; Boyajian et al. 2008; Lane et al. 2001; Demory et al. 2009; Ségransan et al. 2003; Kervella et al. 2008; von Braun et al. 2011). The Yonsei-Yale and Padova isochrones do not match the observations as well as the BCAH and Dartmouth isochrones. The BCAH isochrones are only available in 2 metallicities: $[M/H] = 0.0$ and $[M/H] = -0.5$, necessitating poorly constrained interpolation and extrapolation if used to determine stellar mass and radius. Therefore, we chose to interpolate our T_{eff} and $[M/H]$ measurements of the cool KOIs onto the Dartmouth isochrones. The OLBFI measurements for GJ 205 (Ségransan et al. 2003) do not match any isochrone predictions, and this is likely the result of systematic errors in the OLBFI measurements. We note that in the latest release of *Kepler* planet-candidates, Batalha et al. (2012) confined the stellar parameters of the host stars to the Yonsei-Yale isochrones. This will produce systematically larger radii for the low-mass stars than is evidenced by long-baseline interferometry.

available in two metallicities, $[M/H] = 0.0$ and $[M/H] = -0.5$, and a comprehensive metallicity grid is required for reliable interpolation of our measurements.

All but one of the stars in our sample are treated homogeneously, so the relative radii, masses and temperatures should be precise, even in the presence of model-dependent offsets. There is no model in the Dartmouth isochrones with the same metallicity and effective temperature as KOI 961, so this star is interpolated onto the 5-Gyr BCAH isochrones (see Muirhead et al. 2012, however, for a more detailed analysis of this star). Stellar masses and radii are calculated by interpolation of the main sequence of a 5-Gyr isochrone at the measured total metallicity and effective temperature, illustrated in Figure 4. The assumption of age does not significantly change the results. If very young ages are adopted, the masses and radii typically change only 0.1% between ages of 1 and 10 Gyr, and in all cases significantly less than the reported uncertainties.

We also apply our method to stars with *K*-band measurements in Rojas-Ayala et al. (2012) and radius measurements using optical-long baseline interferometry (see

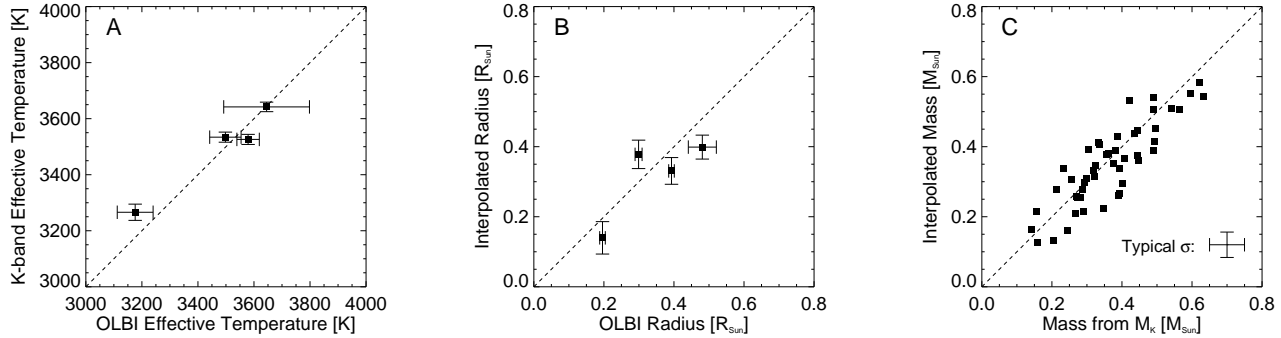


FIG. 3.— Comparison between T_{eff} , R_* , and M_* as measured by optical long-baseline interferometry (OLBI) or the Delfosse et al. (2000) mass- M_K relation (x axes), and the methods used in this paper (y axes) for nearby stars with overlapping measurements. Only 5 stars in Rojas-Ayala et al. (2012) have empirical T_{eff} and R_* measurements in the literature: GJ 699, GJ 411 (both by Lane et al. 2001), GJ 525 (Berger et al. 2006), GJ 581 (von Braun et al. 2011) and GJ 205 (Ségransan et al. 2003). GJ 205 is excluded owing to its aberrant OLBI measurements (see Figure 2). There are 106 stars in Rojas-Ayala et al. (2012) with parallaxes in the literature and 2MASS K -band measurements, allowing for the calculation of M_K and use of the empirically calibrated Delfosse et al. (2000) mass- M_K relation. However, we only include those stars with K -band effective temperatures that are greater than 3200 K (spectral types of M4 and earlier), and we only include stars with parallax measurements larger than 50 mas , amounting to 56 stars. The methods for measuring low-mass star masses and radii employed in this letter are consistent with empirical measurements to within the calculated uncertainties.

Figure 3, Panels B and C). We find good agreement to within the estimated uncertainties.

5. ERROR ANALYSIS

We estimate the uncertainty in the equivalent width, H_2O -K2 index and $[M/H]$ measurements due to noise in the spectra using Monte Carlo simulations. Spextool reports errors for each channel of a reduced spectrum assuming photon noise and read noise in the target and telluric calibrator exposures. For each reduced spectrum, we created 1000 copies, each with random noise added to the spectral channels based on the error reported by Spextool. For each of the 1000 simulations, we measure the Na I and Ca I equivalent widths and H_2O -K2 index. We also calculate $[M/H]$ and T_{eff} , and interpolate those values onto the Dartmouth isochrones. The standard deviations of the quantities across the simulations are taken as the uncertainty in those quantities for a given KOI. All of the resulting distributions are reasonably symmetric, except for the T_{eff} measurements, for which we report asymmetric uncertainties.

The $[M/H]$ and T_{eff} measurements contain additional uncertainty from imperfections in the calibration relation. Possible sources of calibration errors include astrophysical scatter from non-perfect correlation between the indices and $[M/H]$, as well as errors in the relation coefficients due to noise in the calibration spectra. Rojas-Ayala et al. (2012) estimated the calibration errors contribute 0.1 dex of error to $[M/H]$ measurements, based on the root-mean-square residuals in the calibration fit. We estimate a T_{eff} calibration uncertainty of 50 K by comparing the method to OLBI measurements (see Figure 3). We include these uncertainties into the M_* and R_* uncertainty estimates by adding additional Gaussian noise into the $[M/H]$ and T_{eff} measurements of each Monte Carlo iteration with standard deviations of 0.1 and 50 K respectively.

A final uncertainty term arises from the inherent accuracy of the Dartmouth evolutionary isochrones. Figure 3 shows R_* as measured by optical long-baseline interferometry (OLBI) and M_* as measured using the Delfosse et al. (2000) mass- M_K relation, versus mea-

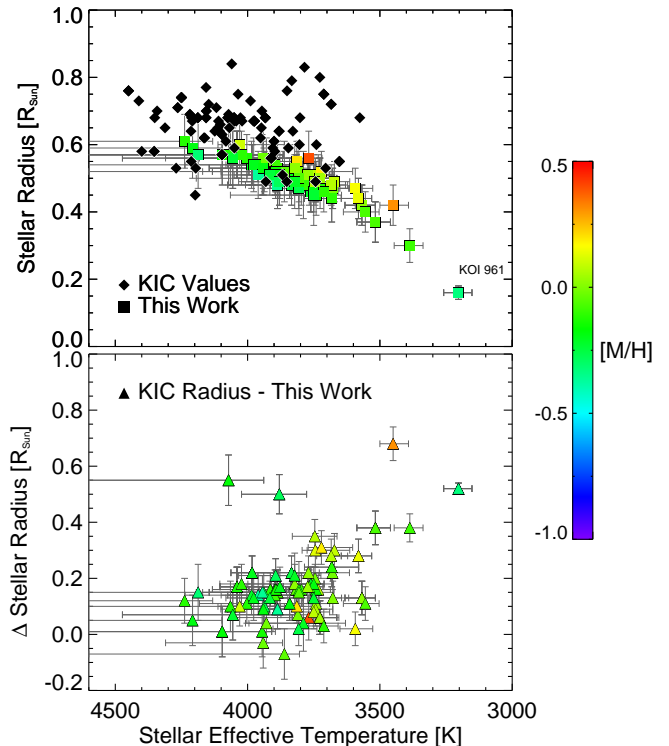


FIG. 4.— Temperature, metallicity and radius determinations for the sample of low-mass KOIs. We use the K -band indices to measure T_{eff} and $[M/H]$, then interpolate those values on the 5-Gyr Dartmouth isochrones to determine stellar mass and stellar radius (Dotter et al. 2008; Feiden et al. 2011). *Top*: Stellar radius vs. T_{eff} . Squares with errorbars are the measurements in this paper and black diamonds are the values from the KIC. *Bot*: The difference between the radius determinations from the KIC and in this work, plotted against our T_{eff} measurements. We dramatically revise the stellar radii of the coolest KOIs. KOI 961 is cooler than the available grid points in the Dartmouth isochrones, so we instead interpolate the T_{eff} and $[M/H]$ onto the 5 Gyr BCAH isochrones Baraffe et al. (1998). KOI 961 is the subject of the third paper in this paper series (Muirhead et al. 2012), wherein we use Barnard’s Star to more accurately estimate its stellar parameters and refit the transit parameters.

measurements made using the Dartmouth interpolations for nearby stars with overlapping measurements in (Rojas-Ayala et al. 2012). We see no evidence for systematic offsets in the Dartmouth interpolations; nevertheless, we add in quadrature an additional uncertainty corresponding to 10% of the interpolated M_* and R_* to the Monte Carlo uncertainties based on the residual differences.

6. RESULTS AND DISCUSSION

Table 1 lists the KOI planet candidates and our measurements of their host star parameters: spectral type, effective temperature, metallicity, and mass and radius, with corresponding uncertainty estimates. We also include our estimate of the planet candidate radii, calculated by applying the R_P/R_* measurements reported in Borucki et al. (2011) to our measurements of R_* . It should be noted that the appropriate limb-darkening coefficient could change as a result of the stellar classification, requiring a more sophisticated calculation of the new planet-candidate radii than in this letter.

Figure 4 plots the effective temperatures, metallicities, masses and radii from our analysis as well as the values in the KIC. Our stellar radii are systematically lower than the values reported in the KIC and, by construction, have better agreement with T_{eff} . The smaller stellar radii imply smaller planet-candidate radii, and many of the revised planet-candidate radii are smaller than 1 Earth radius.

The effective temperatures, radii and masses of the KOIs imply different planet-candidate equilibrium temperature estimates, such that 3 planet-candidates are terrestrial-sized and have equilibrium temperatures

which may permit liquid water to reside on the planet surface, assuming Earth-like albedos and re-radiation fractions. We find that KOIs 463.01, 812.03, and 854.01 are less than $2 R_{\oplus}$ in size with equilibrium temperatures between 215 K and 275 K: rough limits to the habitable zone as calculated by Kasting et al. (1993). Whether liquid water can persist on the surfaces of terrestrial planets orbiting low-mass stars depends strongly on the individual evolution and atmospheric peculiarities of each system, but these KOIs are nevertheless compelling targets for future followup work.

A recent paper by Gaidos et al. (2012) compares the statistics from the M2K M-dwarf Doppler survey (e.g. Apps et al. 2010) with the Kepler results. They found inconsistencies which could be explained if many of the KOI stellar radii were underestimated, a result which is contradictory to our findings. However, the KIC T_{eff} used to compare the M2K and Kepler samples differ from our measurements, and the two samples may have different metallicity distributions.

We would like to thank Michael Cushing for providing us with a version of the Spextool package for the TripleSpec Spectrograph at Palomar. We would also like to thank John Johnson for his thoughtful comments on the letter. The Palomar 200-inch Telescope time was provided by Cornell University. K.R.C. acknowledges support for this work from the Hubble Fellowship Program, provided by NASA through Hubble Fellowship grant HST-HF-51253.01-A awarded by the STScI, which is operated by the AURA, Inc., for NASA, under contract NAS 5-26555.

REFERENCES

- Allard, F., Homeier, D., & Freytag, B. 2011, ArXiv e-prints
 Apps, K., Clubb, K. I., Fischer, D. A., Gaidos, E., Howard, A., Johnson, J. A., Marcy, G. W., Isaacson, H., Giguere, M. J., Valenti, J. A., Rodriguez, V., Chubak, C., & Lepine, S. 2010, PASP, 122, 156
 Baraffe, I., Chabrier, G., Allard, F., & Hauschildt, P. H. 1998, A&A, 337, 403
 Batalha, N. M., Borucki, W. J., Koch, D. G., Bryson, S. T., Haas, M. R., Brown, T. M., Caldwell, D. A., Hall, J. R., Gilliland, R. L., Latham, D. W., Meibom, S., & Monet, D. G. 2010, ApJ, 713, L109
 Batalha, N. M., Rowe, J. F., Bryson, S. T., Barclay, T., Burke, C. J., Caldwell, D. A., Christiansen, J. L., Mullally, F., Thompson, S. E., Brown, T. M., Dupree, A. K., Fabrycky, D. C., Ford, E. B., Fortney, J. J., Gilliland, R. L., Isaacson, H., Latham, D. W., Marcy, G. W., Quinn, S., Ragozzine, D., Shporer, A., Borucki, W. J., Ciardi, D. R., Gautier, III, T. N., Haas, M. R., Jenkins, J. M., Koch, D. G., Lissauer, J. J., Rapin, W., Basri, G. S., Boss, A. P., Buchhave, L. A., Charbonneau, D., Christensen-Dalsgaard, J., Clarke, B. D., Cochran, W. D., Demory, B.-O., Devore, E., Esquerdo, G. A., Everett, M., Fressin, F., Geary, J. C., Girouard, F. R., Gould, A., Hall, J. R., Holman, M. J., Howard, A. W., Howell, S. B., Ibrahim, K. A., Kinemuchi, K., Kjeldsen, H., Klaus, T. C., Li, J., Lucas, P. W., Morris, R. L., Prsa, A., Quintana, E., Sanderfer, D. T., Sasselov, D., Seader, S. E., Smith, J. C., Steffen, J. H., Still, M., Stumpe, M. C., Tarter, J. C., Tenenbaum, P., Torres, G., Twicken, J. D., Uddin, K., Van Cleve, J., Walkowicz, L., & Welsh, W. F. 2012, ArXiv e-prints
 Bean, J. L., Miller-Ricci Kempton, E., & Homeier, D. 2010a, Nature, 468, 669
 Bean, J. L., Seifahrt, A., Hartman, H., Nilsson, H., Wiedemann, G., Reiners, A., Dreizler, S., & Henry, T. J. 2010b, ApJ, 713, 410
 Berger, D. H., Gies, D. R., McAlister, H. A., ten Brummelaar, T. A., Henry, T. J., Sturmann, J., Sturmann, L., Turner, N. H., Ridgway, S. T., Aufdenberg, J. P., & Mérand, A. 2006, ApJ, 644, 475
 Borucki, W. J., Delfosse, X., Udry, S., Forveille, T., Mayor, M., Perrier, C., Bouchy, F., Gillon, M., Lovis, C., Pepe, F., Queloz, D., Santos, N. C., Ségransan, D., & Bertaux, J.-L. 2011, ArXiv e-prints
 Borucki, W. J., Koch, D. G., Basri, G., Batalha, N., Boss, A., Brown, T. M., Caldwell, D., Christensen-Dalsgaard, J., Cochran, W. D., DeVore, E., Dunham, E. W., Dupree, A. K., Gautier, III, T. N., Geary, J. C., Gilliland, R., Gould, A., Howell, S. B., Jenkins, J. M., Kjeldsen, H., Latham, D. W., Lissauer, J. J., Marcy, G. W., Monet, D. G., Sasselov, D., Tarter, J., Charbonneau, D., Doyle, L., Ford, E. B., Fortney, J., Holman, M. J., Seager, S., Steffen, J. H., Welsh, W. F., Allen, C., Bryson, S. T., Buchhave, L., Chandrasekaran, H., Christiansen, J. L., Ciardi, D., Clarke, B. D., Dotson, J. L., Endl, M., Fischer, D., Fressin, F., Haas, M., Horch, E., Howard, A., Isaacson, H., Kolodziejczak, J., Li, J., MacQueen, P., Meibom, S., Prsa, A., Quintana, E. V., Rowe, J., Sherry, W., Tenenbaum, P., Torres, G., Twicken, J. D., Van Cleve, J., Walkowicz, L., & Wu, H. 2011, ApJ, 728, 117
 Boyajian, T. S., McAlister, H. A., Baines, E. K., Gies, D. R., Henry, T., Jao, W.-C., O'Brien, D., Raghavan, D., Touhami, Y., ten Brummelaar, T. A., Farrington, C., Goldfinger, P. J., Sturmann, L., Sturmann, J., Turner, N. H., & Ridgway, S. 2008, ApJ, 683, 424
 Brown, T. M., Latham, D. W., Everett, M. E., & Esquerdo, G. A. 2011, AJ, 142, 112
 Chabrier, G., Gallardo, J., & Baraffe, I. 2007, A&A, 472, L17

- Charbonneau, D., Berta, Z. K., Irwin, J., Burke, C. J., Nutzman, P., Buchhave, L. A., Lovis, C., Bonfils, X., Latham, D. W., Udry, S., Murray-Clay, R. A., Holman, M. J., Falco, E. E., Winn, J. N., Queloz, D., Pepe, F., Mayor, M., Delfosse, X., & Forveille, T. 2009, *Nature*, 462, 891
- Covey, K. R., Lada, C. J., Román-Zúñiga, C., Muench, A. A., Forbrich, J., & Ascenso, J. 2010, *ApJ*, 722, 971
- Croll, B., Albert, L., Jayawardhana, R., Miller-Ricci Kempton, E., Fortney, J. J., Murray, N., & Neilson, H. 2011, *ApJ*, 736, 78
- Cushing, M. C., Rayner, J. T., & Vacca, W. D. 2005, *ApJ*, 623, 1115
- Cushing, M. C., Vacca, W. D., & Rayner, J. T. 2004, *PASP*, 116, 362
- Delfosse, X., Forveille, T., Ségransan, D., Beuzit, J.-L., Udry, S., Perrier, C., & Mayor, M. 2000, *A&A*, 364, 217
- Demory, B.-O., Ségransan, D., Forveille, T., Queloz, D., Beuzit, J.-L., Delfosse, X., di Folco, E., Kervella, P., Le Bouquin, J.-B., Perrier, C., Benisty, M., Duvert, G., Hofmann, K.-H., Lopez, B., & Petrov, R. 2009, *A&A*, 505, 205
- Désert, J.-M., Bean, J., Miller-Ricci Kempton, E., Berta, Z. K., Charbonneau, D., Irwin, J., Fortney, J., Burke, C. J., & Nutzman, P. 2011, *ApJ*, 731, L40+
- Dotter, A., Chaboyer, B., Jevremović, D., Kostov, V., Baron, E., & Ferguson, J. W. 2008, *ApJS*, 178, 89
- Feiden, G. A., Chaboyer, B., & Dotter, A. 2011, *ApJ*, 740, L25
- Gaidos, E., Fischer, D. A., Mann, A. W., & Lépine, S. 2012, *ApJ*, 746, 36
- Girardi, L., Bertelli, G., Bressan, A., Chiosi, C., Groenewegen, M. A. T., Marigo, P., Salasnich, B., & Weiss, A. 2002, *A&A*, 391, 195
- Herter, T. L., Henderson, C. P., Wilson, J. C., Matthews, K. Y., Rahmer, G., Bonati, M., Muirhead, P. S., Adams, J. D., Lloyd, J. P., Skrutskie, M. F., Moon, D., Parshley, S. C., Nelson, M. J., Martinache, F., & Gull, G. E. 2008, in *Society of Photo-Optical Instrumentation Engineers (SPIE) Conference Series*, Vol. 7014, Society of Photo-Optical Instrumentation Engineers (SPIE) Conference Series
- Howard, A. W., Marcy, G. W., Bryson, S. T., Jenkins, J. M., Rowe, J. F., Batalha, N. M., Borucki, W. J., Koch, D. G., Dunham, E. W., Gautier, III, T. N., Van Cleve, J., Cochran, W. D., Latham, D. W., Lissauer, J. J., Torres, G., Brown, T. M., Gilliland, R. L., Buchhave, L. A., Caldwell, D. A., Christensen-Dalsgaard, J., Ciardi, D., Fressin, F., Haas, M. R., Howell, S. B., Kjeldsen, H., Seager, S., Rogers, L., Sasselov, D. D., Steffen, J. H., Basri, G. S., Charbonneau, D., Christiansen, J., Clarke, B., Dupree, A., Fabrycky, D. C., Fischer, D. A., Ford, E. B., Fortney, J. J., Tarter, J., Girouard, F. R., Holman, M. J., Johnson, J. A., Klaus, T. C., Machalek, P., Moorhead, A. V., Morehead, R. C., Ragozzine, D., Tenenbaum, P., Twicken, J. D., Quinn, S. N., Isaacson, H., Shporer, A., Lucas, P. W., Walkowicz, L. M., Welsh, W. F., Boss, A., Devore, E., Gould, A., Smith, J. C., Morris, R. L., Prsa, A., & Morton, T. D. 2011, *ArXiv e-prints*
- Johnson, J. A., Aller, K. M., Howard, A. W., & Crepp, J. R. 2010, *PASP*, 122, 905
- Kasting, J. F., Whitmire, D. P., & Reynolds, R. T. 1993, *Icarus*, 101, 108
- Kervella, P., Mérand, A., Pichon, B., Thévenin, F., Heiter, U., Bigot, L., ten Brummelaar, T. A., McAlister, H. A., Ridgway, S. T., Turner, N., Sturmann, J., Sturmann, L., Goldfinger, P. J., & Farrington, C. 2008, *A&A*, 488, 667
- Kraus, A. L., Tucker, R. A., Thompson, M. I., Craine, E. R., & Hillenbrand, L. A. 2011, *ApJ*, 728, 48
- Kurucz, R. L. The solar spectrum, ed. Cox, A. N., Livingston, W. C., & Matthews, M. S., 663–669
- Lane, B. F., Boden, A. F., & Kulkarni, S. R. 2001, *ApJ*, 551, L81
- Mahadevan, S., Ramsey, L., Wright, J., Endl, M., Redman, S., Bender, C., Roy, A., Zonak, S., Troupe, N., Engel, L., Sigurdsson, S., Wolszczan, A., & Zhao, B. 2010, in *Society of Photo-Optical Instrumentation Engineers (SPIE) Conference Series*, Vol. 7735, Society of Photo-Optical Instrumentation Engineers (SPIE) Conference Series
- Muirhead, P. S., Edelstein, J., Erskine, D. J., Wright, J. T., Muterspaugh, M. W., Covey, K. R., Wishnow, E. H., Hamren, K., Andelson, P., Kimber, D., Mercer, T., Halverson, S. P., Vandenberg, A., Mondo, D., Czeszumaska, A., & Lloyd, J. P. 2011, *PASP*, 123, 709
- Muirhead, P. S., Johnson, J. A., Apps, K., Carter, J. A., Morton, T. D., Fabrycky, D. C., Pineda, J. S., Bottom, M., Rojas-Ayala, B., Schlawin, E., Hamren, K., Covey, K. R., Crepp, J. R., Stassun, K. G., Pepper, J., Hebb, L., Kirby, E. N., Howard, A. W., Isaacson, H. T., Marcy, G. W., Levitan, D., Diaz-Santos, T., Armus, L., & Lloyd, J. P. 2012, *ApJ*, 747, 144
- Nordström, B., Mayor, M., Andersen, J., Holmberg, J., Pont, F., Jørgensen, B. R., Olsen, E. H., Udry, S., & Mowlavi, N. 2004, *A&A*, 418, 989
- Nutzman, P. & Charbonneau, D. 2008, *PASP*, 120, 317
- Rayner, J. T., Cushing, M. C., & Vacca, W. D. 2009, *ApJS*, 185, 289
- Ribas, I. 2006, *Ap&SS*, 304, 89
- Rojas-Ayala, B., Covey, K. R., Muirhead, P. S., & Lloyd, J. P. 2010, *ApJ*, 720, L113
- . 2012, *ApJ*, 748, 93
- Ségransan, D., Kervella, P., Forveille, T., & Queloz, D. 2003, *A&A*, 397, L5
- Torres, G. 2007, *ApJ*, 671, L65
- . 2011, *ArXiv e-prints*
- Vacca, W. D., Cushing, M. C., & Rayner, J. T. 2003, *PASP*, 115, 389
- Valenti, J. A. & Fischer, D. A. 2005, *ApJS*, 159, 141
- van Belle, G. T. & von Braun, K. 2009, *ApJ*, 694, 1085
- von Braun, K., Boyajian, T. S., Kane, S. R., van Belle, G. T., Ciardi, D. R., López-Morales, M., McAlister, H. A., Henry, T. J., Jao, W.-C., Riedel, A. R., Subasavage, J. P., Schaefer, G., ten Brummelaar, T. A., Ridgway, S., Sturmann, L., Sturmann, J., Mazingue, J., Turner, N. H., Farrington, C., Goldfinger, P. J., & Boden, A. F. 2011, *ApJ*, 729, L26
- Yi, S. K., Kim, Y.-C., & Demarque, P. 2003, *ApJS*, 144, 259

TABLE 1
COOL KOI STELLAR HOST AND PLANET CANDIDATE PROPERTIES

KOI	– Borucki et al. (2011) – Transit Parameters		– <i>K</i> -Band Stellar Measurements – (This Work)			– Dartmouth Stellar Interpolants – (This Work)		– New Planet Parameters – (This Work)		
	P [days]	R_P/R_*	T_{eff} [K]	[M/H] ^a	Sp. Type	M_* [M_\odot]	R_* [R_\odot]	a [AU]	R_P [R_\oplus]	$T_{\text{eq,P}}$ [K] ^b
104.01	2.5080910 ± 1.3e-05	0.035 ± 4.8e-03	4238 ⁺⁴⁵⁹ ₋₁₀₆	-0.12 ± 0.10	M0V	0.64 ± 0.08	0.61 ± 0.08	0.03106 ± 1.29e-03	2.32 ± 0.43	827
156.01	8.0414400 ± 1.3e-04	0.023 ± 1.3e-02	3983 ⁺⁸⁰ ₋₈₁	-0.20 ± 0.10	M0V	0.56 ± 0.06	0.54 ± 0.06	0.06482 ± 2.35e-03	1.36 ± 0.78	508
156.02	5.1885600 ± 1.2e-04	0.020 ± 1.4e-02	0.04840 ± 1.75e-03	1.18 ± 0.84	588
156.03	11.7761793 ± 5.4e-05	0.033 ± 2.8e-04	0.08358 ± 3.03e-03	1.95 ± 0.22	447
222.01	6.3123822 ± 5.8e-05	0.033 ± 3.9e-04	4096 ⁺⁵³⁸ ₋₁₈₇	-0.17 ± 0.11	M0V	0.59 ± 0.09	0.57 ± 0.09	0.05611 ± 2.81e-03	2.05 ± 0.31	576
222.02	12.7939701 ± 3.0e-04	0.026 ± 6.5e-04	0.08987 ± 4.50e-03	1.62 ± 0.25	455
227.01	17.6607609 ± 2.5e-04	0.040 ± 3.9e-04	3745 ⁺⁵¹ ₋₅₉	-0.02 ± 0.10	M1V	0.49 ± 0.06	0.47 ± 0.05	0.10496 ± 3.91e-03	2.06 ± 0.24	350
247.01	13.8152399 ± 3.2e-04	0.031 ± 1.1e-03	3741 ⁺⁵⁴ ₋₅₁	0.03 ± 0.10	M1V	0.51 ± 0.06	0.49 ± 0.06	0.08992 ± 3.29e-03	1.64 ± 0.20	383
248.01	7.2034941 ± 6.5e-05	0.039 ± 5.5e-04	3816 ⁺¹⁴¹ ₋₅₄	-0.05 ± 0.11	M1V	0.54 ± 0.06	0.51 ± 0.06	0.05929 ± 2.27e-03	2.18 ± 0.27	495
248.02	10.9140100 ± 1.8e-04	0.034 ± 1.1e-03	0.07821 ± 3.00e-03	1.90 ± 0.24	431
248.03	2.5765359 ± 3.3e-05	0.027 ± 1.2e-02	0.02987 ± 1.14e-03	1.51 ± 0.70	697
250.01	12.2823563 ± 9.7e-05	0.049 ± 4.8e-04	3887 ⁺²⁵⁸ ₋₅₇	-0.08 ± 0.11	M0V	0.55 ± 0.08	0.53 ± 0.08	0.08551 ± 3.93e-03	2.83 ± 0.40	427
250.02	17.2520409 ± 2.5e-04	0.049 ± 1.5e-03	0.10725 ± 4.93e-03	2.83 ± 0.41	381
250.03	3.5438709 ± 7.1e-05	0.017 ± 1.0e-03	0.03734 ± 1.72e-03	0.98 ± 0.15	646
251.01	4.1643710 ± 2.3e-05	0.044 ± 5.0e-04	3810 ⁺⁶⁴ ₋₆₅	-0.02 ± 0.10	M1V	0.54 ± 0.06	0.52 ± 0.06	0.04124 ± 1.51e-03	2.47 ± 0.28	594
252.01	17.6043892 ± 2.4e-04	0.042 ± 2.2e-02	3743 ⁺⁶³ ₋₆₅	0.06 ± 0.11	M1V	0.51 ± 0.06	0.49 ± 0.06	0.10593 ± 4.00e-03	2.24 ± 1.20	354
253.01	6.3832402 ± 7.1e-05	0.043 ± 7.9e-04	3769 ⁺⁵⁹ ₋₅₀	0.40 ± 0.13	M1V	0.59 ± 0.08	0.56 ± 0.08	0.05633 ± 2.49e-03	2.62 ± 0.36	524
254.01	2.4552391 ± 1.6e-06	0.184 ± 1.2e-03	3814 ⁺¹²⁴ ₋₅₄	0.20 ± 0.11	M1V	0.58 ± 0.07	0.55 ± 0.06	0.02967 ± 1.12e-03	11.11 ± 1.30	727
255.01	27.5215607 ± 3.1e-04	0.045 ± 4.7e-04	3770 ⁺⁶⁶ ₋₇₈	0.02 ± 0.11	M1V	0.53 ± 0.06	0.51 ± 0.06	0.14469 ± 5.52e-03	2.50 ± 0.30	312
256.01	1.3786809 ± 1.2e-05	0.123 ± 2.3e-03	3450 ⁺⁵⁰ ₋₅₈	0.31 ± 0.10	M3V	0.43 ± 0.06	0.42 ± 0.06	0.01833 ± 8.10e-04	5.60 ± 0.76	726
314.01	13.7810497 ± 1.6e-04	0.029 ± 5.8e-04	3841 ⁺⁵⁰ ₋₅₁	-0.18 ± 0.10	M1V	0.52 ± 0.06	0.50 ± 0.06	0.09060 ± 3.24e-03	1.58 ± 0.18	398
314.02	23.0904007 ± 3.4e-04	0.023 ± 3.9e-02	0.12781 ± 4.56e-03	1.26 ± 2.13	335
430.01	12.3764496 ± 1.9e-04	0.038 ± 1.8e-02	3797 ⁺⁹⁸ ₋₅₈	-0.10 ± 0.11	M1V	0.51 ± 0.06	0.48 ± 0.06	0.08346 ± 3.25e-03	2.00 ± 0.98	403
438.01	5.9312038 ± 7.0e-05	0.030 ± 1.6e-02	3985 ⁺²⁵¹ ₋₆₄	-0.22 ± 0.11	M0V	0.56 ± 0.08	0.54 ± 0.07	0.05288 ± 2.27e-03	1.76 ± 0.97	560
448.01	10.1396103 ± 2.3e-04	0.030 ± 9.4e-04	3894 ⁺⁹⁷ ₋₉₈	-0.28 ± 0.11	M0V	0.52 ± 0.06	0.50 ± 0.06	0.07369 ± 2.84e-03	1.64 ± 0.21	448
448.02	43.6204987 ± 1.3e-03	0.049 ± 8.8e-03	0.19491 ± 7.52e-03	2.68 ± 0.58	275
463.01	18.4781704 ± 1.9e-04	0.047 ± 9.2e-04	3387 ⁺⁵⁹ ₋₅₀	-0.09 ± 0.10	M3V	0.30 ± 0.05	0.30 ± 0.05	0.09116 ± 5.22e-03	1.52 ± 0.26	269
478.01	11.0234518 ± 8.5e-05	0.051 ± 1.8e-03	3744 ⁺⁵⁰ ₋₆₁	0.13 ± 0.10	M1V	0.52 ± 0.06	0.50 ± 0.06	0.07812 ± 2.80e-03	2.78 ± 0.33	418
494.01	25.6971893 ± 6.7e-04	0.031 ± 2.4e-02	3789 ⁺²¹⁹ ₋₁₅₉	-0.21 ± 0.16	M1V	0.50 ± 0.10	0.48 ± 0.10	0.13495 ± 8.57e-03	1.61 ± 1.29	314
500.01	7.0534778 ± 8.3e-05	0.034 ± 5.4e-04	4040 ⁺⁶⁴ ₋₁₇₅	-0.14 ± 0.11	M0V	0.59 ± 0.07	0.57 ± 0.07	0.06022 ± 2.34e-03	2.10 ± 0.26	546
500.02	9.5216999 ± 1.4e-04	0.035 ± 2.3e-02	0.07355 ± 2.86e-03	2.16 ± 1.44	494
500.03	3.0721660 ± 4.6e-05	0.018 ± 7.4e-04	0.03460 ± 1.34e-03	1.11 ± 0.14	720
500.04	4.6453528 ± 6.7e-05	0.026 ± 2.3e-02	0.04558 ± 1.77e-03	1.60 ± 1.43	628
500.05	0.9867790 ± 1.2e-05	0.015 ± 1.4e-02	0.01623 ± 6.30e-04	0.93 ± 0.87	1052
503.01	8.2223597 ± 1.0e-04	0.034 ± 6.5e-04	4003 ⁺¹⁷⁹ ₋₇₅	-0.13 ± 0.11	M0V	0.58 ± 0.07	0.56 ± 0.07	0.06633 ± 2.63e-03	2.06 ± 0.25	511
531.01	3.6874621 ± 8.9e-06	0.055 ± 7.6e-03	4030 ⁺⁸² ₋₁₆₉	0.10 ± 0.10	M0V	0.62 ± 0.08	0.60 ± 0.07	0.03990 ± 1.55e-03	3.59 ± 0.66	689
571.01	7.2673302 ± 1.3e-04	0.024 ± 1.5e-02	3761 ⁺⁷⁷ ₋₅₀	-0.21 ± 0.11	M1V	0.48 ± 0.06	0.46 ± 0.06	0.05763 ± 2.23e-03	1.21 ± 0.77	470
571.02	13.3433104 ± 1.5e-04	0.028 ± 6.7e-04	0.08642 ± 3.34e-03	1.41 ± 0.17	384
571.03	3.8867581 ± 3.8e-05	0.026 ± 7.0e-03	0.03797 ± 1.47e-03	1.31 ± 0.39	579
596.01	1.6827060 ± 1.4e-05	0.026 ± 4.2e-04	3678 ⁺⁵² ₋₅₀	0.00 ± 0.10	M1V	0.49 ± 0.06	0.47 ± 0.06	0.02188 ± 8.60e-04	1.34 ± 0.16	753
605.01	2.6281440 ± 2.0e-05	0.028 ± 4.4e-04	3941 ⁺³⁶⁹ ₋₇₃	-0.03 ± 0.16	M0V	0.58 ± 0.09	0.56 ± 0.09	0.03101 ± 1.56e-03	1.70 ± 0.26	736
610.01	14.2824602 ± 2.6e-04	0.027 ± 8.4e-04	3679 ⁺⁵⁰ ₋₆₄	-0.02 ± 0.10	M1V	0.49 ± 0.06	0.47 ± 0.06	0.09066 ± 3.60e-03	1.37 ± 0.17	368
663.01	2.7556019 ± 1.7e-05	0.025 ± 6.5e-03	3834 ⁺⁵⁰ ₋₅₇	-0.25 ± 0.10	M1V	0.51 ± 0.06	0.48 ± 0.06	0.03068 ± 1.12e-03	1.32 ± 0.38	672
663.02	20.3070793 ± 2.9e-04	0.023 ± 4.3e-04	0.11617 ± 4.26e-03	1.22 ± 0.14	345

TABLE 1 — *Continued*

KOI	– Borucki et al. (2011) –	– <i>K</i> -Band Stellar Measurements –				– Dartmouth Stellar Interpolants –		– New Planet Parameters –		
	Transit Parameters	(This Work)	(This Work)	(This Work)	(This Work)	(This Work)	(This Work)	(This Work)	(This Work)	
	P [days]	R_P/R_*	T_{eff} [K]	[M/H] ^a	Sp. Type	M_* [M_\odot]	R_* [R_\odot]	a [AU]	R_P [R_\oplus]	$T_{\text{eq,P}}$ [K] ^b
676.01	7.9725132 ± 7.6e-05	0.059 ± 3.4e-03	3914 ⁺⁸² ₋₅₉	-0.12 ± 0.10	M0V	0.55 ± 0.06	0.53 ± 0.06	0.06406 ± 2.29e-03	3.39 ± 0.43	495
676.02	2.4532239 ± 2.3e-05	0.039 ± 8.6e-04	0.02920 ± 1.04e-03	2.24 ± 0.26	734
736.01	18.7952309 ± 6.0e-04	0.036 ± 3.8e-02	3682 ⁺¹⁰³ ₋₁₀₂	-0.11 ± 0.14	M1V	0.46 ± 0.08	0.44 ± 0.07	0.10714 ± 5.54e-03	1.74 ± 1.86	330
736.02	6.7388001 ± 2.1e-04	0.026 ± 1.1e-03	0.05407 ± 2.80e-03	1.26 ± 0.21	465
739.01	1.2870520 ± 1.2e-05	0.027 ± 5.1e-04	3733 ⁺⁷⁶ ₋₅₉	0.07 ± 0.11	M1V	0.53 ± 0.06	0.51 ± 0.06	0.01873 ± 7.00e-04	1.49 ± 0.18	856
775.01	16.3852291 ± 7.0e-04	0.029 ± 1.6e-03	3898 ⁺¹⁷⁷ ₋₇₇	-0.09 ± 0.12	M0V	0.56 ± 0.07	0.54 ± 0.07	0.10379 ± 4.44e-03	1.69 ± 0.24	390
775.02	7.8776102 ± 1.8e-04	0.033 ± 1.2e-03	0.06370 ± 2.72e-03	1.93 ± 0.27	499
778.01	2.2433400 ± 3.6e-05	0.028 ± 1.0e-03	3741 ⁺¹⁴⁰ ₋₅₄	-0.16 ± 0.12	M1V	0.47 ± 0.06	0.45 ± 0.06	0.02612 ± 1.10e-03	1.38 ± 0.19	686
781.01	11.5982304 ± 1.5e-04	0.050 ± 2.9e-02	3672 ⁺¹⁰³ ₋₅₈	0.09 ± 0.12	M1V	0.51 ± 0.06	0.49 ± 0.06	0.08015 ± 3.24e-03	2.66 ± 1.58	399
784.01	19.2693005 ± 5.9e-04	0.032 ± 3.3e-02	3767 ⁺¹³⁵ ₋₅₁	-0.10 ± 0.11	M1V	0.51 ± 0.06	0.48 ± 0.06	0.11210 ± 4.43e-03	1.69 ± 1.76	345
812.01	3.3402400 ± 3.5e-05	0.039 ± 2.8e-02	3887 ⁺¹⁸⁸ ₋₇₈	-0.36 ± 0.12	M0V	0.51 ± 0.07	0.48 ± 0.07	0.03487 ± 1.57e-03	2.06 ± 1.50	638
812.02	20.0608597 ± 4.7e-04	0.035 ± 1.1e-03	0.11521 ± 5.18e-03	1.84 ± 0.27	351
812.03	46.1851006 ± 1.9e-03	0.034 ± 1.7e-03	0.20087 ± 9.03e-03	1.79 ± 0.27	266
817.01	23.9715996 ± 1.1e-03	0.033 ± 2.0e-03	3750 ⁺⁶⁶ ₋₆₀	0.08 ± 0.11	M1V	0.54 ± 0.06	0.51 ± 0.06	0.13215 ± 4.89e-03	1.84 ± 0.24	325
818.01	8.1142902 ± 1.3e-04	0.040 ± 2.1e-02	3721 ⁺⁵⁰ ₋₁₁₈	0.19 ± 0.12	M1V	0.54 ± 0.07	0.52 ± 0.06	0.06455 ± 2.56e-03	2.27 ± 1.22	466
854.01	56.0517006 ± 2.7e-03	0.036 ± 1.6e-03	3593 ⁺⁵⁸ ₋₆₆	0.16 ± 0.11	M2V	0.49 ± 0.06	0.47 ± 0.06	0.22599 ± 9.31e-03	1.83 ± 0.25	227
868.01	234.0000000 ± 1.4e+01	0.161 ± 2.5e-03	3822 ⁺¹⁷⁷ ₋₅₈	0.02 ± 0.12	M1V	0.55 ± 0.07	0.53 ± 0.07	0.60896 ± 2.50e-02	9.27 ± 1.20	157
870.01	5.9121299 ± 1.7e-04	0.030 ± 1.3e-03	4072 ⁺⁷²⁰ ₋₁₃₃	-0.17 ± 0.11	M0V	0.59 ± 0.10	0.57 ± 0.09	0.05375 ± 2.91e-03	1.86 ± 0.32	583
870.02	8.9859695 ± 2.7e-04	0.028 ± 8.9e-04	0.07106 ± 3.84e-03	1.73 ± 0.29	507
875.01	4.2209358 ± 2.7e-05	0.044 ± 3.4e-04	3861 ⁺⁷³⁹ ₋₅₇	-0.05 ± 0.13	M0V	0.55 ± 0.10	0.52 ± 0.09	0.04183 ± 2.32e-03	2.51 ± 0.43	602
877.01	5.9548702 ± 1.0e-04	0.034 ± 2.6e-02	3896 ⁺²³⁷ ₋₅₀	-0.20 ± 0.11	M0V	0.54 ± 0.07	0.52 ± 0.07	0.05220 ± 2.21e-03	1.92 ± 1.49	541
877.02	12.0395698 ± 3.4e-04	0.031 ± 1.1e-03	0.08347 ± 3.53e-03	1.75 ± 0.24	428
886.01	8.0128098 ± 1.6e-04	0.035 ± 4.0e-02	3726 ⁺⁶⁹ ₋₇₁	-0.12 ± 0.11	M1V	0.49 ± 0.06	0.47 ± 0.06	0.06190 ± 2.46e-03	1.80 ± 2.07	453
898.01	9.7705898 ± 1.8e-04	0.041 ± 3.7e-02	3893 ⁺¹⁰² ₋₉₅	-0.15 ± 0.11	M0V	0.54 ± 0.07	0.52 ± 0.06	0.07295 ± 2.84e-03	2.34 ± 2.13	460
898.02	5.1699100 ± 1.1e-04	0.033 ± 3.2e-02	0.04773 ± 1.86e-03	1.88 ± 1.84	569
898.03	20.0892296 ± 5.4e-04	0.034 ± 4.1e-02	0.11796 ± 4.59e-03	1.94 ± 2.35	362
899.01	7.1138802 ± 1.1e-04	0.028 ± 1.9e-02	3568 ⁺⁶⁴ ₋₅₁	0.02 ± 0.10	M2V	0.44 ± 0.06	0.42 ± 0.06	0.05504 ± 2.38e-03	1.28 ± 0.89	435
899.02	3.3065691 ± 3.9e-05	0.021 ± 6.6e-04	0.03303 ± 1.43e-03	0.96 ± 0.13	562
899.03	15.3681297 ± 2.6e-04	0.029 ± 3.6e-02	0.09198 ± 3.98e-03	1.33 ± 1.66	336
901.01	12.7325573 ± 4.6e-05	0.074 ± 5.4e-04	3945 ⁺⁸¹¹ ₋₅₀	-0.14 ± 0.11	M0V	0.56 ± 0.10	0.54 ± 0.09	0.08792 ± 4.87e-03	4.36 ± 0.73	431
902.01	83.9041977 ± 1.7e-03	0.080 ± 6.6e-04	3960 ⁺¹⁴⁰ ₋₁₃₃	-0.37 ± 0.12	M0V	0.53 ± 0.07	0.51 ± 0.07	0.30300 ± 1.34e-02	4.41 ± 0.62	225
912.01	10.8484697 ± 2.7e-04	0.037 ± 3.1e-02	4208 ⁺¹⁰⁶⁷ ₋₁₁₁	-0.19 ± 0.11	M0V	0.61 ± 0.10	0.59 ± 0.09	0.08145 ± 4.33e-03	2.40 ± 2.04	501
936.01	9.4678946 ± 8.3e-05	0.044 ± 4.6e-04	3581 ⁺⁶⁵ ₋₅₀	0.14 ± 0.10	M2V	0.46 ± 0.06	0.44 ± 0.06	0.06753 ± 2.77e-03	2.12 ± 0.27	404
936.02	0.8930440 ± 4.4e-06	0.026 ± 1.1e-02	0.01399 ± 5.70e-04	1.25 ± 0.55	887
947.01	28.5989094 ± 5.7e-04	0.040 ± 9.3e-04	3750 ⁺⁵⁶ ₋₇₅	-0.18 ± 0.11	M1V	0.49 ± 0.06	0.46 ± 0.06	0.14388 ± 5.66e-03	2.02 ± 0.25	296
952.01	5.9012551 ± 7.6e-05	0.037 ± 6.7e-04	3727 ⁺¹⁰⁴ ₋₆₄	0.04 ± 0.13	M1V	0.52 ± 0.07	0.50 ± 0.06	0.05151 ± 2.06e-03	2.02 ± 0.26	512
952.02	8.7524595 ± 1.5e-04	0.038 ± 1.1e-02	0.06699 ± 2.68e-03	2.08 ± 0.65	449
952.03	22.7803307 ± 3.1e-04	0.040 ± 9.3e-04	0.12676 ± 5.07e-03	2.18 ± 0.28	326
952.04	2.8960290 ± 6.3e-05	0.019 ± 1.5e-03	0.03205 ± 1.28e-03	1.04 ± 0.15	650
961.01 ^c	1.2137721 ± 4.4e-06	0.053 ± 3.3e-03	3203 ⁺⁵⁶ ₋₅₁	-0.33 ± 0.10	M4V	0.14 ± 0.02	0.16 ± 0.02	0.01153 ± 5.50e-04	0.92 ± 0.14	526
961.02	0.4532880 ± 9.0e-07	0.194 ± 8.1e-04	0.00598 ± 2.80e-04	3.38 ± 0.46	730
961.03	1.8651130 ± 9.1e-06	0.140 ± 2.3e-01	0.01535 ± 7.30e-04	2.44 ± 4.02	456
1024.01	5.7477322 ± 6.5e-05	0.026 ± 8.2e-04	3937 ⁺¹⁶³ ₋₆₁	-0.27 ± 0.11	M0V	0.53 ± 0.07	0.52 ± 0.06	0.05097 ± 1.99e-03	1.47 ± 0.19	554
1026.01	94.1023026 ± 9.7e-03	0.024 ± 8.0e-04	3773 ⁺⁵⁸ ₋₆₁	0.03 ± 0.10	M1V	0.54 ± 0.06	0.51 ± 0.06	0.32898 ± 1.20e-02	1.34 ± 0.16	208
1078.01	3.3536820 ± 2.9e-05	0.035 ± 1.0e-03	3807 ⁺⁹⁷ ₋₆₉	-0.26 ± 0.15	M1V	0.49 ± 0.07	0.47 ± 0.06	0.03460 ± 1.49e-03	1.79 ± 0.25	617

TABLE 1 — *Continued*

KOI	– Borucki et al. (2011) –	– <i>K</i> -Band Stellar Measurements –			– Dartmouth Stellar Interpolants –		– New Planet Parameters –			
	Transit Parameters	(This Work)	(This Work)	(This Work)	(This Work)	(This Work)	(This Work)	(This Work)	(This Work)	
	P [days]	R_P/R_\star	T_{eff} [K]	[M/H] ^a	Sp. Type	M_\star [M_\odot]	R_\star [R_\odot]	a [AU]	R_P [R_\oplus]	$T_{\text{eq,P}}$ [K] ^b
1085.01	7.7179398 ± 2.3e-04	0.017 ± 1.9e-03	3939 ⁺²³¹ ₋₈₆	-0.25 ± 0.12	M0V	0.54 ± 0.08	0.52 ± 0.07	0.06219 ± 2.78e-03	0.97 ± 0.17	503
1141.01	5.7279601 ± 1.5e-04	0.027 ± 1.2e-03	4065 ⁺⁵⁷⁷ ₋₁₃₇	-0.13 ± 0.11	M0V	0.59 ± 0.09	0.57 ± 0.09	0.05268 ± 2.65e-03	1.69 ± 0.27	591
1146.01	7.0969501 ± 2.0e-04	0.024 ± 4.4e-02	3555 ⁺⁸³ ₋₅₂	-0.07 ± 0.11	M2V	0.41 ± 0.06	0.40 ± 0.06	0.05383 ± 2.51e-03	1.04 ± 1.91	425
1152.01	4.7222500 ± 8.6e-06	0.269 ± 3.0e-03	3806 ⁺⁵⁰ ₋₆₄	-0.13 ± 0.10	M1V	0.52 ± 0.06	0.49 ± 0.06	0.04421 ± 1.64e-03	14.45 ± 1.69	560
1164.01	2.8011279 ± 8.8e-05	0.015 ± 5.5e-04	3684 ⁺⁵⁵ ₋₆₂	0.07 ± 0.10	M1V	0.51 ± 0.06	0.48 ± 0.06	0.03102 ± 1.20e-03	0.79 ± 0.10	642
1176.01	1.9737610 ± 1.0e-06	0.157 ± 2.9e-04	3806 ⁺³⁸⁸ ₋₁₃₂	-0.06 ± 0.19	M1V	0.53 ± 0.11	0.50 ± 0.11	0.02491 ± 1.66e-03	8.64 ± 1.82	756
1201.01	2.7575290 ± 4.6e-05	0.026 ± 2.8e-03	3712 ⁺⁸⁵ ₋₅₄	-0.11 ± 0.11	M1V	0.48 ± 0.06	0.46 ± 0.06	0.03013 ± 1.21e-03	1.30 ± 0.22	638
1202.01	0.9283080 ± 1.5e-05	0.027 ± 8.5e-04	4894 ⁺⁶⁰⁷ ₋₉₀₄	-0.06 ± 0.12	M0V	0.76 ± 0.12	0.72 ± 0.11	0.01703 ± 8.80e-04	2.12 ± 0.34	1403
1266.01	11.4194403 ± 2.0e-04	0.027 ± 6.2e-04	3822 ⁺²¹² ₋₉₉	-0.21 ± 0.12	M1V	0.51 ± 0.08	0.49 ± 0.08	0.07932 ± 4.08e-03	1.45 ± 0.24	419
1298.01	11.0082302 ± 1.3e-04	0.044 ± 7.9e-03	5189 ⁺⁹⁹ ₋₇₉₈	-0.37 ± 0.14	K7V	0.76 ± 0.12	0.72 ± 0.11	0.08852 ± 4.28e-03	3.44 ± 0.80	651
1361.01	59.8791008 ± 1.1e-03	0.034 ± 7.2e-04	3929 ⁺⁶⁶ ₋₁₃₅	-0.02 ± 0.11	M0V	0.57 ± 0.07	0.55 ± 0.07	0.24861 ± 9.64e-03	2.04 ± 0.25	258
1403.01	18.7540894 ± 5.1e-04	0.028 ± 5.7e-02	3977 ⁺¹⁰⁵ ₋₁₈₄	-0.20 ± 0.12	M0V	0.56 ± 0.08	0.54 ± 0.08	0.11380 ± 5.20e-03	1.65 ± 3.38	382
1404.01	6.6620498 ± 2.6e-04	0.024 ± 3.6e-02	3750 ⁺³¹⁵ ₋₁₀₅	-0.23 ± 0.15	M1V	0.48 ± 0.10	0.45 ± 0.09	0.05409 ± 3.40e-03	1.19 ± 1.80	479
1408.01	14.5345097 ± 3.9e-04	0.022 ± 9.5e-04	4023 ⁺⁸² ₋₁₁₃	-0.11 ± 0.10	M0V	0.59 ± 0.07	0.57 ± 0.07	0.09751 ± 3.63e-03	1.36 ± 0.17	427
1422.01	5.8416181 ± 7.1e-05	0.038 ± 4.1e-02	3517 ⁺⁷⁰ ₋₅₇	-0.07 ± 0.11	M2V	0.38 ± 0.06	0.37 ± 0.06	0.04595 ± 2.34e-03	1.53 ± 1.67	439
1422.02	19.8503704 ± 3.8e-04	0.036 ± 1.3e-03	0.10386 ± 5.29e-03	1.45 ± 0.23	292
1422.03	3.6213870 ± 9.3e-05	0.025 ± 1.6e-03	0.03341 ± 1.70e-03	1.01 ± 0.17	515
1427.01	2.6130109 ± 4.1e-05	0.021 ± 9.8e-04	3878 ⁺¹⁷³ ₋₇₅	-0.20 ± 0.11	M0V	0.53 ± 0.07	0.51 ± 0.07	0.03003 ± 1.30e-03	1.16 ± 0.17	702
1459.01	0.6920230 ± 1.3e-06	0.075 ± 1.0e-03	3746 ⁺⁸⁵ ₋₈₄	0.07 ± 0.12	M1V	0.51 ± 0.07	0.49 ± 0.06	0.01222 ± 5.00e-04	3.98 ± 0.51	1043
1475.01	1.6093230 ± 2.4e-05	0.026 ± 1.3e-03	4056 ⁺⁴¹⁷ ₋₂₃₄	-0.23 ± 0.13	M0V	0.57 ± 0.10	0.56 ± 0.09	0.02234 ± 1.18e-03	1.58 ± 0.27	894
1475.02	9.5124798 ± 2.5e-04	0.032 ± 1.5e-03	0.07302 ± 3.84e-03	1.95 ± 0.33	494
1515.01	1.9370290 ± 2.1e-05	0.018 ± 5.6e-04	3944 ⁺⁸⁰ ₋₆₀	-0.36 ± 0.10	M0V	0.52 ± 0.06	0.51 ± 0.06	0.02452 ± 8.80e-04	0.99 ± 0.12	790
1577.01	2.8062129 ± 6.0e-05	0.022 ± 1.5e-03	3940 ⁺¹⁶¹ ₋₁₁₈	-0.18 ± 0.12	M0V	0.55 ± 0.08	0.53 ± 0.08	0.03191 ± 1.47e-03	1.28 ± 0.20	710
1584.01	5.8708401 ± 1.5e-04	0.025 ± 1.1e-03	4187 ⁺⁹⁹⁹ ₋₂₅₅	-0.32 ± 0.14	M0V	0.59 ± 0.11	0.57 ± 0.10	0.05345 ± 3.02e-03	1.56 ± 0.28	604
1588.01	3.5174849 ± 4.5e-05	0.000 ± 1.8e+00	3916 ⁺⁸⁶ ₋₆₈	-0.24 ± 0.10	M0V	0.53 ± 0.06	0.51 ± 0.06	0.03670 ± 1.36e-03	0.00 ± 0.00	643
1596.01	5.9236002 ± 1.3e-04	0.021 ± 2.2e-02	3880 ⁺¹⁴³ ₋₁₀₃	-0.28 ± 0.12	M0V	0.51 ± 0.07	0.49 ± 0.07	0.05132 ± 2.27e-03	1.12 ± 1.19	529
1596.02	105.3551025 ± 3.9e-03	0.032 ± 7.1e-02	0.34966 ± 1.55e-02	1.71 ± 3.81	202

^a Metallicity measurements for stars earlier than M0 ($T_{\text{eff}} \lesssim 4000$ K) represent an extrapolation of the Rojas et al (2012) M dwarf [M/H] calibration.

^b The planetary equilibrium temperatures ($T_{\text{eq,P}}$) were calculated assuming an Earth-like albedo and re-radiation fraction for each planet-candidate. We do not include uncertainty estimates for $T_{\text{eq,P}}$ due to the ambiguity of those assumptions.

^c There is no model in the Dartmouth isochrones with the same [M/H] and T_{eff} as KOI 961, so this star is interpolated onto the 5-Gyr BCAH isochrones. See Muirhead et al. (2012) for a more detailed analysis of this star.